

**ignedNCSX**  
Design Basis Analysis

Non-Linear Modular Coil Analysis

NCSX-CALC-14-007

21 July 2007

**Prepared by:**

---

K. Freudenberg, ORNL

*I have reviewed this calculation and, to my professional satisfaction, it is properly performed and correct. I concur with analysis methodology and inputs and with the reasonableness of the results and their interpretation.*

**Reviewed by:**

---

D Williamson, ORNL Engineer

<p>Controlled Document <b>THIS IS AN UNCONTROLLED DOCUMENT ONCE PRINTED.</b> Check the NCSX Engineering Web prior to use to assure that this document is current.</p>
---

**Table Of Contents**

**I. Executive Summary .....3**

**II. Introduction .....3**

**III. ANALYSIS APPROACH .....4**

*II.A. Assumptions .....4*

*II.B. Material Properties .....4*

*II.C Magnetic Loading.....5*

*II.D. Analysis Methodology .....5*

*II.E. ANSYS Mesh .....7*

*II.F. NCSX Modular Coil Analysis Capabilities .....8*

*Software and data files .....10*

*Drawings and models .....10*

*Material properties .....10*

**III. RESULTS .....11**

*Clamp stresses .....15*

*III.c. High stress regions.....15*

*III.d. Mod Coil Toroidal Flange Connections .....18*

**IV. CONCLUSIONS AND FUTURE WORK.....21**

**REFERENCES .....22**

**Appendix A: Reaction Forces on MCWF from TF-Induced Loads .....23**

**Appendix B: Consideration of using one bolt on inner leg to get total shear load:.....26**

**Appendix C Stresses Near Area of Clamp 63 on C Coil (DEMO of stress plots at every clamp.).....32**

## I. Executive Summary

The purpose of this analysis is to examine the structural characteristics of the NCSX modular coil shell and windings. A non-linear FEA study has been performed on the modular coils of the National Compact Stellarator Experiment (NCSX). The modular coils provide the primary magnetic field within NCSX and consist of flexible cable conductor wound on a cast and machined winding form and vacuum impregnated with epoxy. Eighteen coils and associated winding forms are connected at assembly into a toroidal shell structure. The ANSYS® model, includes the complete shell structure of all three coils and contact regions allow the winding to slide and detach form the shell structure. The winding pack is thus restrained only by the clamps. The purpose of this study was to evaluate the structural response of the windings and shell structure during cooldown and normal operation.

## II. Introduction

The function of the NCSX modular coil system is 1) to provide specified quasi-axisymmetric magnetic field configurations, 2) to provide access for tangential neutral beam injection (NBI), radio frequency (RF) heating, and diagnostics, and 3) to provide a robust mechanical structure that minimizes non-symmetric field errors. The coil set consists of three field periods with six coils per period, for a total of 18 coils. Due to stellarator symmetry, only three different coil shapes are needed to make up the complete coil set. The coils are connected electrically in three circuits according to type, and as such can produce alternate magnetic configurations by independently varying the current for each type.

The modular coils are wound onto stainless steel castings that are then bolted together to form a structural shell. As shown in Fig. 1, the winding cavity is a “tee” structure that is located on and integral with the plasma side of the shell. During operation, electromagnetic forces push the windings outward against the shell and laterally toward the “tee”, so that only intermittent clamps are required for structural support.

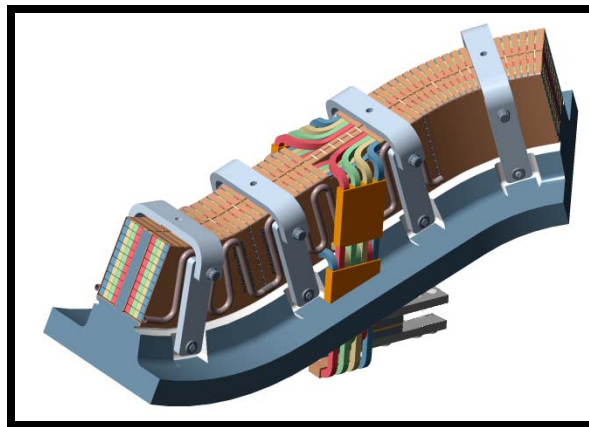


Fig. 1. Mod Coil Schematic showing the winding cavity (tee), winding and clamps

This primary focus of this analysis is to acquire a proper understanding of how the coil set will react structurally when loaded with the magnetic field. In contrast to the linear analysis, as documented in Myatt [1], this analysis allows the winding packs to slide on the coil via frictionless contact surfaces. The stresses, strains and potential winding/shell gap

displacements are central in determining whether the structure is within the design criteria as stated in by Reiersen [2]. The deformed winding coil shape calculated by the analysis will also be used as a physics tool to verify that the magnetic field

### III. ANALYSIS APPROACH

The geometry of the shell and modular coil structures renders any global stress analysis performed by hand as a virtual impossibility. Thus, the approach taken in this report was to perform a series of finite element models and compare and contrast the answers for both the linear and non-linear cases where the winding slips along the tee..

#### II.A. Assumptions

1. Material properties evaluated at 77 K.
2. Winding packs are modeled with isotropic material properties.
3. 60 - degree "anti-cyclic symmetry" on edge flange faces based on the 3 coil shell model (A,B,C).
4. Non-linear sliding between tee and winding pack is frictionless.
5. Clamps are only used on winding packs that are free to move against the shell.

#### II.B. Material Properties

The properties used assumed that the shell is made of stainless steel and the coil windings consist of a homogeneous copper/epoxy mixture. The properties are listed in Table 1. The thermal properties are shown in Table 2. These values are used where when the thermal loading from a localized modular coil model is applied to the shell and the winding form.

TABLE I: Material Properties.

	E (Mpa)	CTE /K	Poisson's Ratio
Tee/shell	151,000.00	0.00E+00	0.31
Modular Coil	58,600.00	1.00E-05	0.3
Toroidal Spacer	151,000.00	0.00E+00	0.31
poloidal spacer	151,000.00	0.00E+00	0.31
Wing bag	1,100.00	2.30E-04	0.42
Wing bag	1,100.00	2.30E-04	0.32
Clamp	151,000.00	0.00E+00	0.31
Top pad	21.28	1.25E-03	0

TABLE II: Material Properties.

<b>Cp (J/kg K)</b>	80 K	100 K	150 K	200 K
Winding cable	171.4	212.3	270.1	300.7
Cu Cooling Plate	205.1	255.3	324.1	359
Insulation	348.9	413.7	537	626.8
SS Tee	215.3	275.5	362.1	416.4
glue	348.9	413.7	537	626.8
<b>K (W/m K)</b>	80 K	100 K	150 K	200 K
Winding cable (x, y direction)	7.5	7.5	7.5	7.5
Winding cable (z direction)	300	300	300	300
Cu Cooling Plate	529.3	461.5	418.1	407
Insulation	0.227	0.252	0.396	0.322
glue (4 * insulation)	0.91	1.01	1.58	1.29
SS Tee	8.114	9.224	11.17	12.63
<b>Density (kg/m<sup>3</sup>)</b>	80 K -200K			
Winding cable	7028			
Cu Cooling Plate	8900			
Insulation	1200			
SS Tee	8030			
glue	1200			

### II.C Magnetic Loading

Calculations to determine the fields and forces acting on all of the stellarator core magnets have been completed for seven reference operating scenarios. The worst case for determining forces in the modular coils appears to be the 2T high beta scenario at time=0.197-s. Two independent field calculations have been performed, one with the ANSYS [3] code and the other with MAGFOR [4]. A comparison of magnetic flux density at 2-T indicates that the models are in good agreement, with only a 4% difference in peak field due primarily to mesh and integration differences. TF loads are also applied to the global model on the support legs of the modular coil winding form (See Appendix A).

### II.D. Analysis Methodology

The conductor experiences about 0.04 % shrinkage more than the shell when being cooled down to 85 K. This differential strain value was utilized through the coefficient of thermal expansion and a known temperature change. Example: strain =  $-400\mu\epsilon$ , arbitrary temp difference = 72 F. Therefore, Winding cte =  $-400\mu\epsilon / 72 F = -5.55E-6 / ^\circ F$ , Tee cte =  $0 / ^\circ F$ . Thus, by applying a global temperature change to the model, an imposed strain was exerted between the winding and the tee. The preload on the clamp pads was imposed in a similar manner.

The complete shell structure of all three coils, was studied with the FEA program ANSYS. The model uses stellarator symmetry and constant equations for the edge flange restraints (shown below in Fig.3). One node on the B shell is restrained

in the vertical direction (z) to complete the required DOF constraints. The magnetic forces are calculated directly as nodal forces in the Ansys Electromagnetic Solver. Thus, the averaging errors derived from converting MAGFOR Electromagnetic load output to discrete pressure areas have been eliminated. Contact regions defined in ANSYS allow the winding to slide and detach from the shell structure. A prototypical clamp has been placed over the clamp pads attached to the top of the tee, which more closely models the real world behavior of the clamp.

The ANSYS model runs three coils at a time with only one coil free to slide. Thus, for each run, only one set of clamps is needed to solve. By running the coils “in-turn”, the models are able to converge to a solution in a reasonable amount of time. Running a multiple contact problem with all three coils sliding is not currently solvable. Other components have been included in the Ansys solution. These include, wing shims, (modeled as an epoxy/glass composite) which brace the wings against their opposing shell and edge flange shims which connect the three shell types together. The wing shims on the CC and AA flanges were not included. In a separate linear analysis by Len Myatt, he showed that there was little benefit to adding the wing shims given the complexity involved relating to writing the constraint equations and adjacent contact elements. In general, the supported C-wing configuration reduces the maximum stress and deformation in the coil C WP (83MPa vs. 70 MPa for unrestrained and restrained respectively), but has minimal effect on the MCWP maximum stress .

Figure 2 shows the hierarchy of how the eventual non-linear solution is derived. The ProE models are first simplified by removing obvious mesh consuming features such as bolt holes and rounds in some places. Next, the model is fed into Mechanical so that the winding packs can be broken into regions which can be sweep meshed for the Ansys magnetic solver. The model is then transferred into workbench where it is meshed and the material properties are defined. This is also where the contact regions are defined between the windings and the shell structure. The model is then transferred to classical Ansys and the associatively with the ProE is lost. Here, only nodes, elements material properties, components and any loading are transferred to Ansys classical. The solid CAD data, i.e. volumes areas, lines and key-points, is not currently transferred from workbench to ANSYS classic.

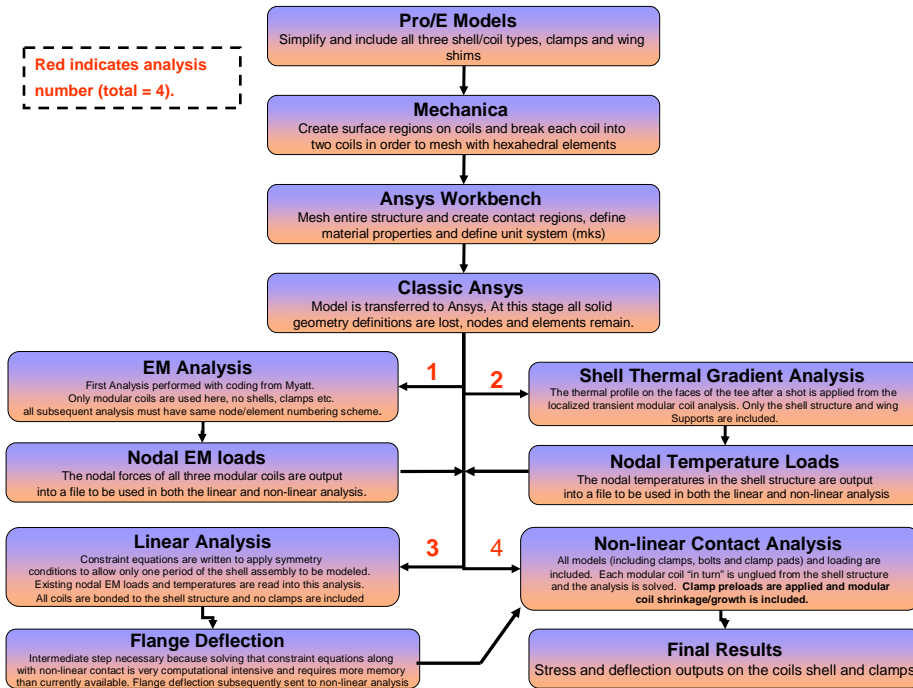


Fig 2: Hierarchy for solving the non-linear contact analysis for the NCSX half period assembly

## II.E. ANSYS Mesh

The ANSYS Mesh (shown in Fig. 3) consists of both tetrahedral shell elements and hexahedral coil elements. Bonded contact surfaces are used to join all parts together. The contact surfaces between the windings and the shell structure are set to a frictionless option so that the coil may be “slippery” and slide along the length of the coil, as well as open up gaps from the shell. Although some features have been suppressed in the shell, namely bolts holes on the flanges, there are many intricate details that are incorporated in the shell structure. These include the tee relief groove, port holes, poloidal break and various other chamfers, rounds and cuts which provide for a very robust model and mesh. The winding pack mesh consists of a 2 X 6 element formulation with an average element length of 2.3 cm. Latter revisions have included the bolt holes to determine the stress on each individual bolted joint region and the shear loading over the flange face.. Originally, the three coil structure was meshed as one body encompassing the three coils and four shims. Today, each has its own material properties, real constants and key-opts.

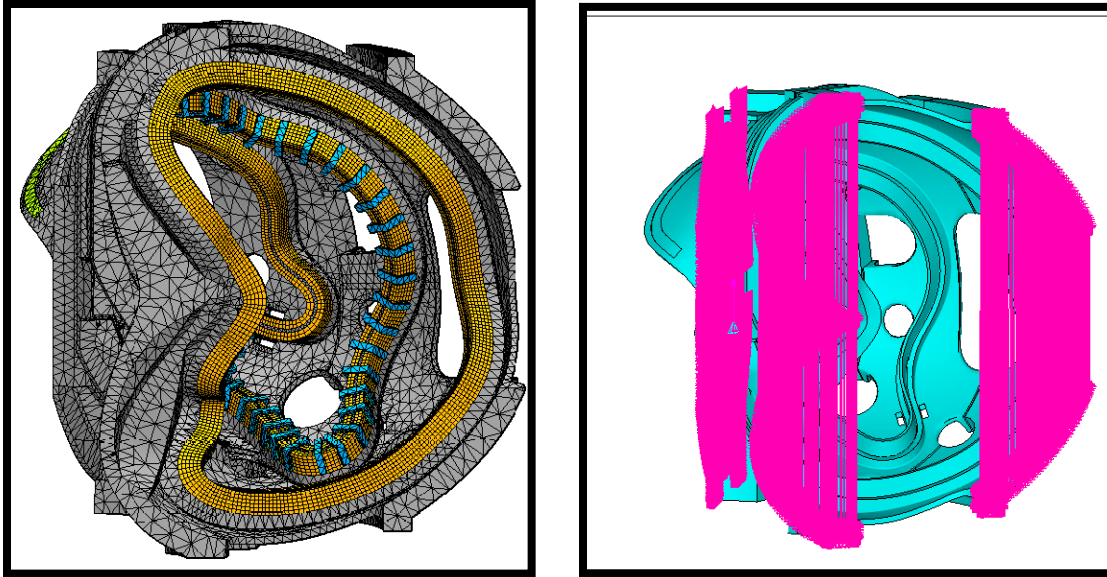


Fig. 3. Right) Mesh of the overall assembly model including clamps on Coil B. Left) Constraint equations connecting the top and bottom of the AA and CC flanges.

#### II.F. NCSX Modular Coil Analysis Capabilities

- 4 Different Magnetic Loading Scenarios (0.5 T, 1.7T Ohmic/ $t=0.0s$ , or 2.0T HighBeta/ $t=0.0s$ , or 320kA Ohmic/ $t=0.206s$ , or 2.0T HighBeta/ $t=0.197s$ ). Fig.4 shows the EM model and corresponding forces.
- Thermal shrinkage/growth of winding pack as the winding pack will shrink away during curing and during pulse.
- Thermal gradient in shell due to heating of winding pack during/after pulse. This is shown in Fig 5. and Fig 6. below. A transient thermal model of a simple winding pack (straight) was run with full detail of the conductors and turn wrap insulation, which illustrated the thermal contours of the shell after a 15 minute cool down period. These thermal restraints were then placed on the global model and Fig 6. shows excellent agreement between the two models near the tee region. Finally, Fig 7 shows the thermal load applied to the entire 3 coil shell model as a steady state solution. This illustrates the predicted thermal distribution between 15 minute shots. These thermal loads are then superimposed and read into the structural model when it runs. It was found that they have a minimal effect on the results.
- Non-linear contact as the coils can “in turn” separate and slide along the shell structure. This requires three separate runs of the analysis code for each coil.
- Clamps are included in the non-linear model and are modeled according to the current clamp design.
- Preloads using ANSYS pretension elements can be applied to both the clamps bolts (a few at a time)
- Preloads can be applied to the Belleville washers in the clamp assembly using the cte of the washer material to push against the clamp and winding.
- Symmetry conditions are applied via constraint equations on the outer flanges in the linear model. This allows only one half period of the model to be analyzed (six coils and three shells)



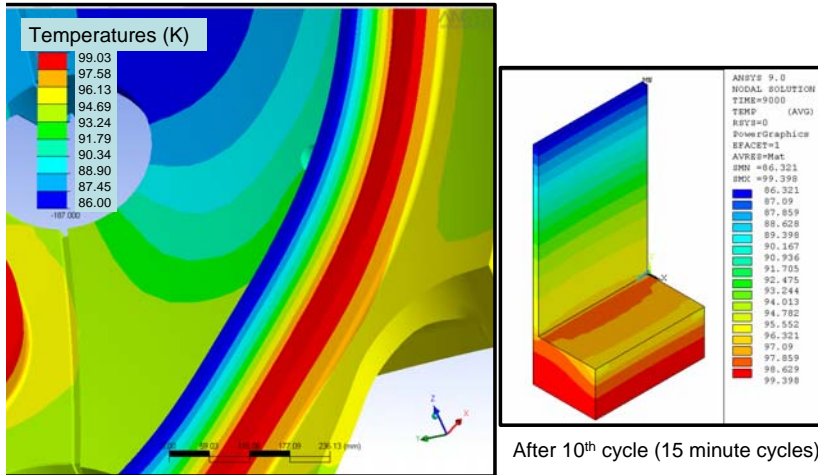


Fig 6: Variation of temperature distribution in the shell of the modular coil after the thermal profile (right image) is mapped onto the castings.

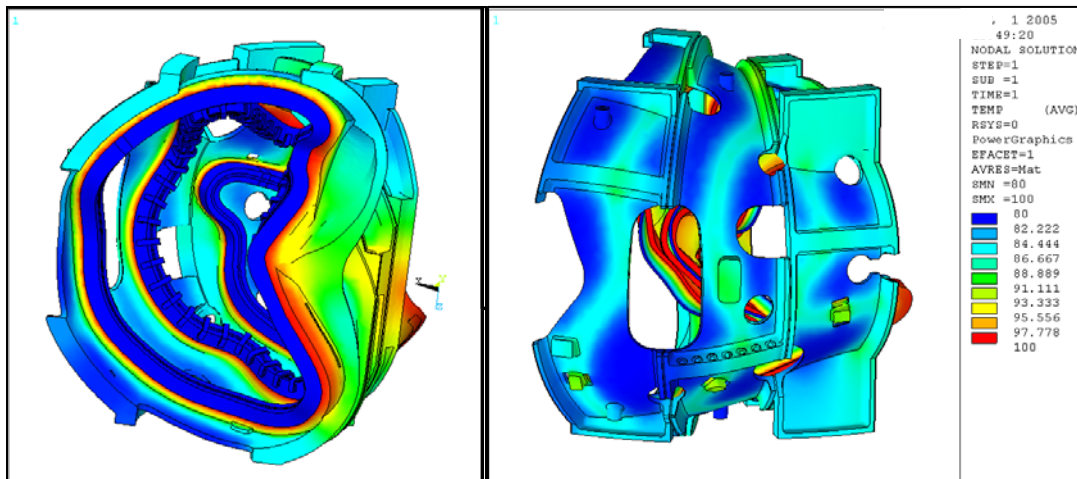


Fig 7: Castings and Windings (left image) Castings only Thermal variation. Reference temperature is 80 K.

#### Software and data files

The model is constructed in Ansys 9.0-11.0 and all of the preprocessing and post processing is done within the Ansys classic environment.

#### Drawings and models

No drawings have been referenced in this study. All models have been created as .cdb and .db files.

#### Material properties

The temperature dependent material properties are above listed in Table 1. For clarification, the insulation is the material that surrounds the winding cable and the glue is the material that is used to connect the copper cladding layers together and used in the “crimp” joints. Also, for modeling and meshing purposes it is necessary to model the glue as thicker than it is in reality, otherwise an extremely large mesh will result. The glue is 0.2” thick in the model and is approximately 0.05” in reality, thus the conductivity has been multiplied by 4 to account for this scaling factor.

### III. RESULTS

Table 1 summarizes the stress results from both FEA programs (Ansys and Mechanica for each respective study). Initially, the analyst used Mechanica when first examining the structure in 2003. The Mechanica shell stress reported is for the supporting tee structure only as the entire shell was not able to be modeled in that program. The max stresses occur in relatively the same spots on the windings even though the two models are restrained differently. The lone max stress that exceeds 83 MPa is the coil C run on Mechanica. This stress, upon closer inspection, is more than likely an overestimate as the max stresses is due to the tee base being rigidly constrained at its base. Compared to the ANSYS analysis where the tee is attached directly to the shell and not rigidly fixed, the stress in the same region is 76 MPa.

TABLE III. Stress Results for both winding and shell for 2T case. (Von Mises Stress Reported in all cases)

Coil	Max Winding Stress (MPa)	Max Shell Stress (MPa)
Mechanica A	72	170 (Tee)
Mechanica B	79	269 (Tee)
Mechanica C	89	221 (Tee)
Ansys A	79	231
Ansys B	66	283
Ansys C	76	227

Table 3 summarizes the max gap deflections and strains that each model predicts. The gap indicated in the table is the predicted maximum separation that will occur between the winding and the tee based on the non linear contact algorithms. The shell deflection presented for the Mechanica runs only include the deflection on the web of the tee sine the model is restrained on the back of the tee, thus a direct comparison between the two models based on this criterion cannot be easily made. The trend for maximum gap deflection holds for booth the analysis programs as the gap increases from A to and B to C in both programs with coil C experiencing the largest gap of 0.6 -0.8 mm. The maximum gap for the non-linear ANSYS run of coil B is shown below in Fig. 8, which is indicative of how the gaps in the other models appeared near the extreme wing turns.

TABLE IV: Principle Strains and global deformations.

Case/Coil	Max Principal Strain (mm/mm)	Winding Shell Gap (mm)	Max Shell Deflection (mm)
Mechanica A	0.0011	0.09	0.24 (Tee)
Mechanica B	0.0012	0.58	0.76 (Tee)
Mechanica C	0.0015	0.8	0.36 (Tee)
Ansys A	0.0013	0.2	1.4
Ansys B	0.0010	0.5	2.6
Ansys C	0.0012	0.6	1.4

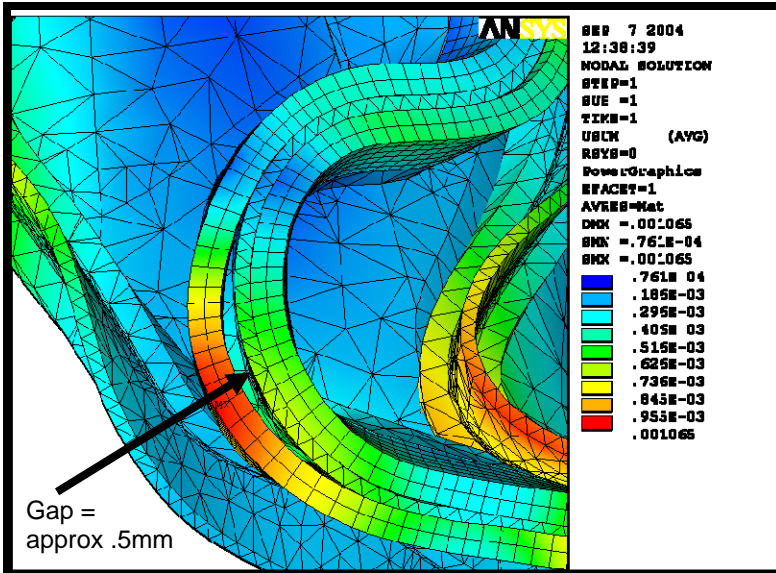


Fig. 8. Winding/shell Gap of approximately 0.5 mm located on the extreme turn of the wing of the modular coil B.

The maximum principle strains for the two B coil runs are compared in Figure 9. The maximum principle strain occurs on the extreme interior of the wing regions in both cases. The Ansys model has a higher average strain along its outboard edges as the coil is being moved by the shell which itself is deforming due to the magnetic loads.

The Von Mises Stress distribution for the shell structure is shown in Fig. 10. The max stress occurs near the wing interests between shells B and C. The peak stress on the tee structure of coil B is about 175 MPa. Fig. 11 indicates the degree of which the shell will globally deform due to the electromagnetic loads with a maximum deformation of 2.2 mm occurring on the web of the tee holding the slippery coil. The max deformation of all three non-linear models occurred on the tee of the coil that was free to move out and along the shell. Fig 12. shows the global deflection of the twelve coils (a half period) with a peak movement 2.18 mm occurring on the two B coils near the same location as the deflection on the B shell tee.

According to the specification of casting shell, Ref. [6], the minimum 0.2% yield strength and the tensile strength to be 496.4 GPa and 655 GPa, respectively. The allowable is the less of 1/2 tensile strength or 2/3 yield strength. Thus, the allowable stress would be 322.5 MPa, which is higher than the maximum von Mises stress of 283 Mpa listed in this report.

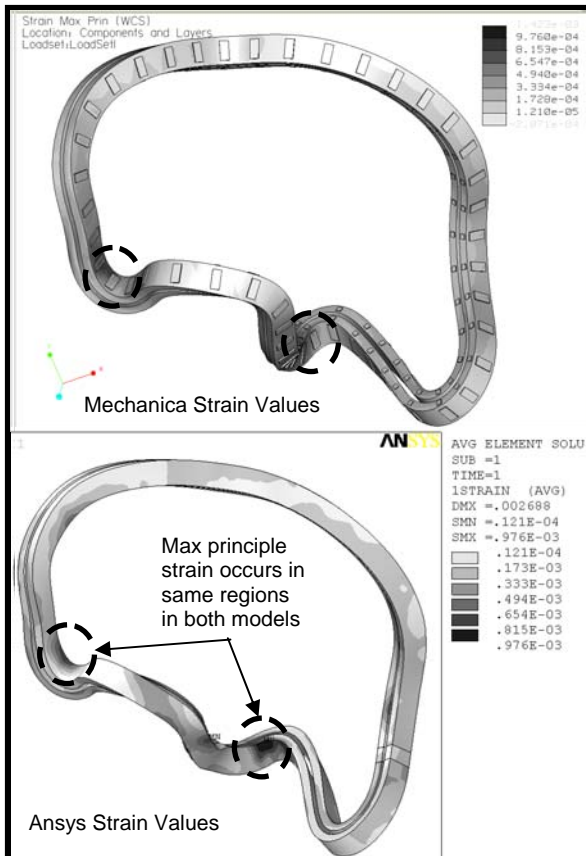


Fig. 9. Strain Values for winding pack B for both Mechanica and Ansys setups.

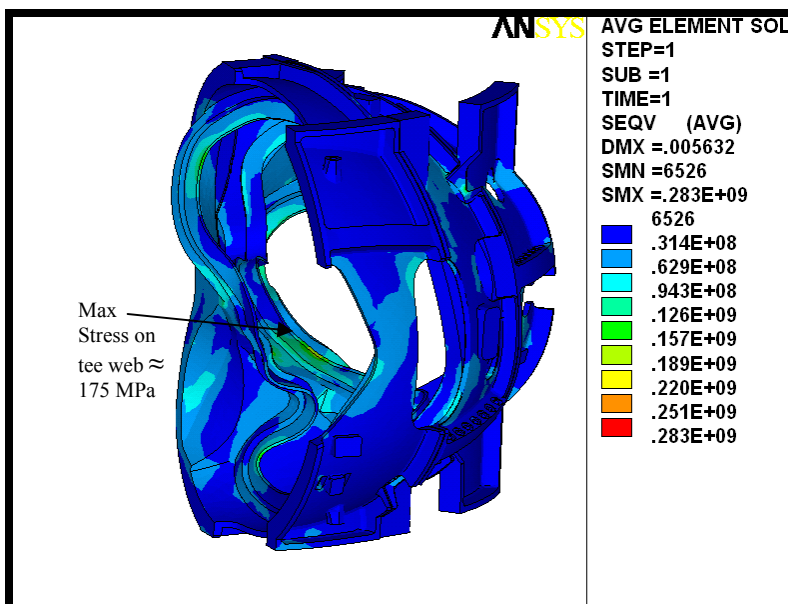


Fig. 10. Von Mises Stress Distribution for the shell structure. Max Stress (283 Mpa) occurs at joint region geometric discontinuity between shell flanges, Max Web tee stress  $\approx$  175 Mpa..

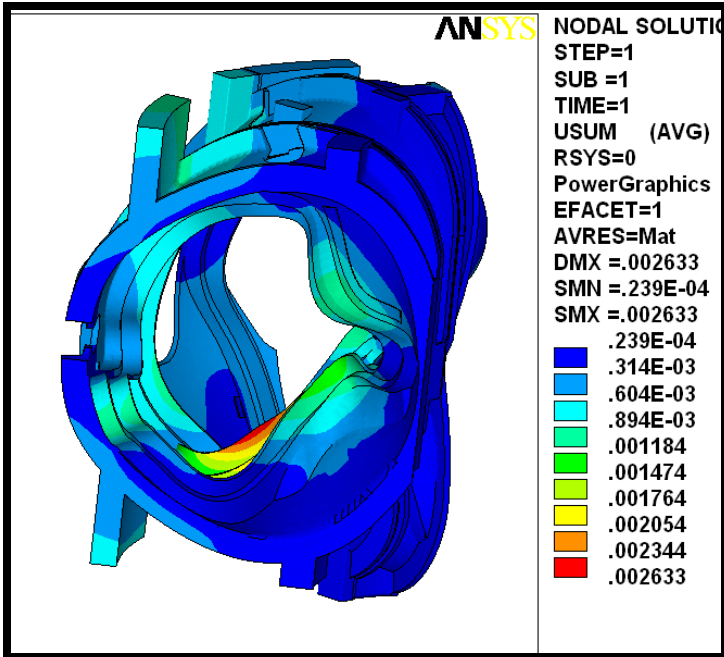


Fig. 11. Shell Deformation for a “slippery” coil B.

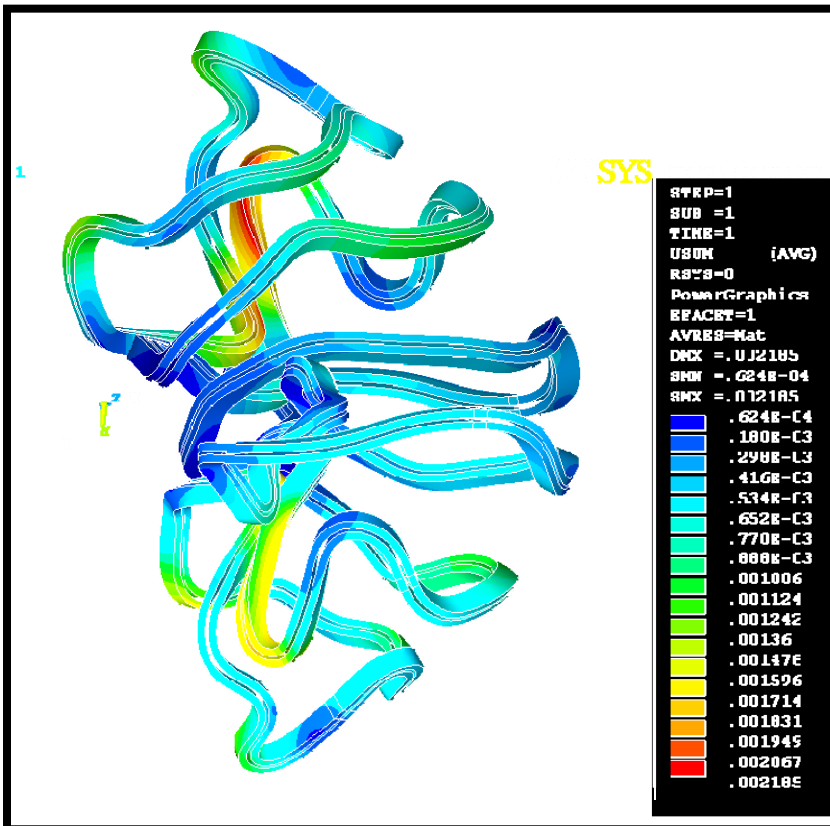


Fig 12: Deflections of coils for non-linear analysis

## Clamp stresses

The clamps shown in this report are simplistic in that they do not model all of the connecting components in detail. The clamps are preloaded by applying a thermal expansion to the pads separating them from the winding forms. Figure 13 displays the Von Mises contour plot of the coil type B clamp pattern. High stresses are found at the interfaces of clamps and the tee because of the rigid bonded connection there. High stresses are primarily caused by the bending moments and the shear forces that are primarily induced by the lateral movement of the coils. The maximum Von Mises stress is 247 MPa at the clamp-tee interface. The actual stresses should be much smaller once sliding and rotational effects are allowed for in the model.

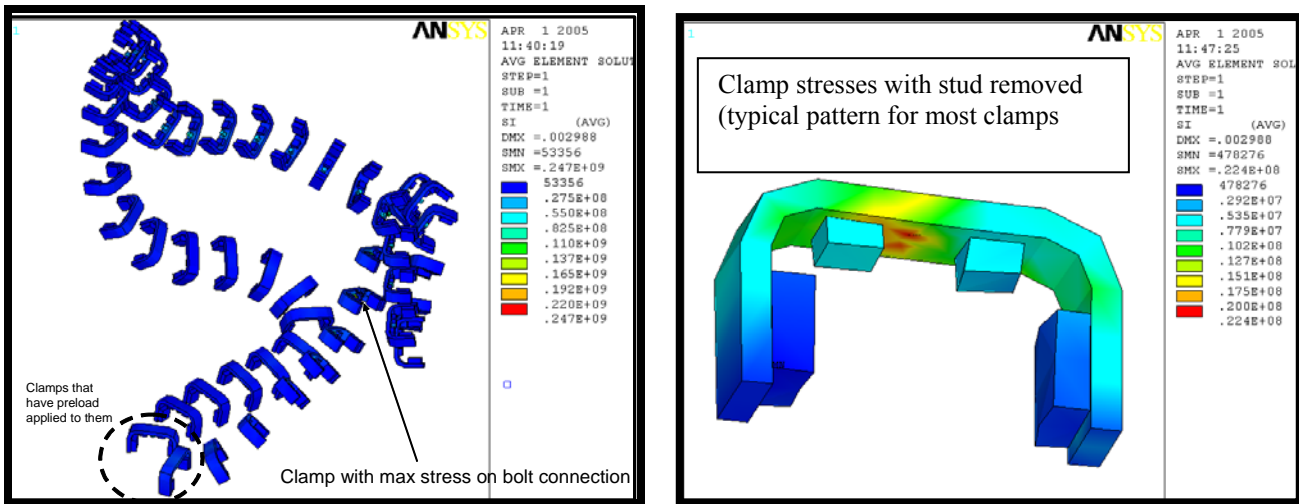


Fig 13: Stresses (Intensity) on clamps

### III.c. High stress regions

Figure 14, Figure 15, Figure 16, and Figure 17 identify the relative high stress areas on each coil type. They illustrate a numbering scheme for the 3/8-16UNC tapped holes in the tee. Per the proposal of Major Tool, every tenth hole shall be identified by etching. The high stress region shall be identified as the web of the “tee” cross-section.

Detailed stress plots have been produced at every clamp location, which helped to determine the exact location of the higher stress regions. A demo of the stress script is shown in Appendix C.



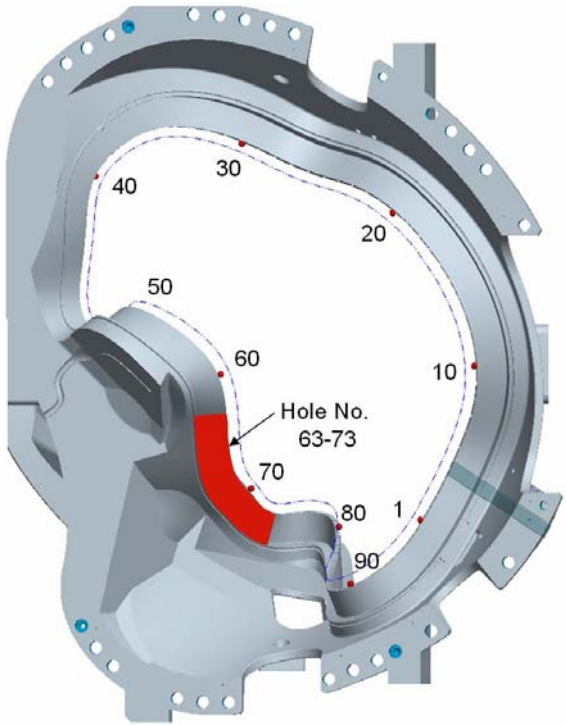


Fig. 16 High Stress Region Identification for Type-B MCWF

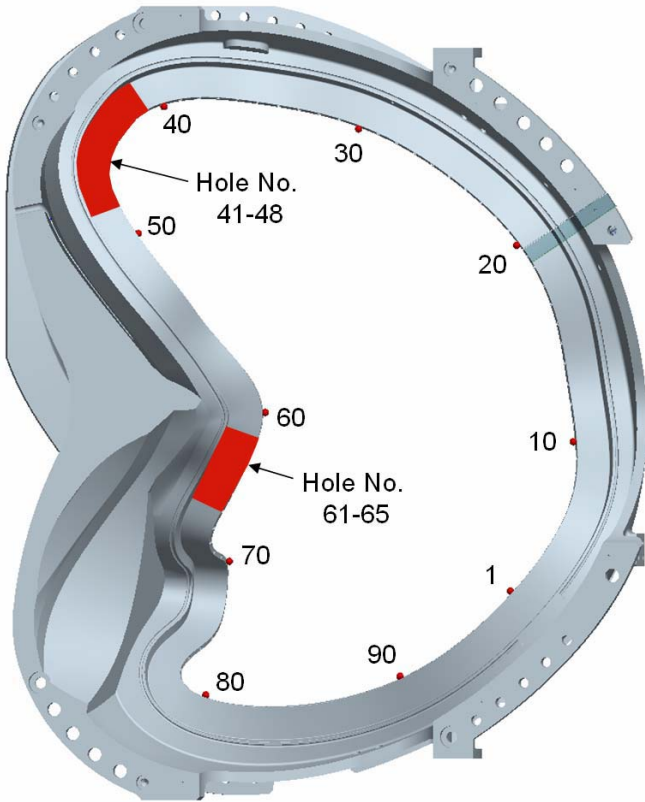


Fig. 17 High Stress Region Identification for Type-A MCWF

### III.d. Mod Coil Toroidal Flange Connections

This model does not include any bolt or bolt preloads on the toroidal flange joints. This will be covered in a future analysis report where we will include the bolt, preload and friction on each of these joints. Here, all coils and shims are boned/glued together. Fig 14 - Fig. 17 show the shear and normal stresses for each of the interfaces. The top set of pictures is the PPPL Fan [7] images of the their NCSX global analysis. There is quite good agreement between the two models on these comparison figures. The same contour scales have been used for direct comparison. Looking at the normal compression plots below, one can see that the flange is in both compression and tension and that there is no clear compressional force on the inboard leg that could restrain it by friction alone. Thus, of particular concern, is the area that is unbolted on each of the flanges as it experiences a large amount of shear with no preload/ bolt connection to react it. After a considerable amount of discussion and an exhaustive study of inboard restraint options, it was decided to weld the inboard legs together for the AA, AB and BC joints. Further, additional inner leg bolts will be added to the CC interface. The weld analysis and the CC inner leg bolt analysis are essentially spin offs of this analysis as they use the same magnetic forces, TF coil loading, and restraints as this model. These separate spin-offs will show that the welds and bolts do adequately address the shear problem over the entire flanges face of the toroidal shims. Thus, the issue of slippage and shear loads on the inner leg has been resolved.

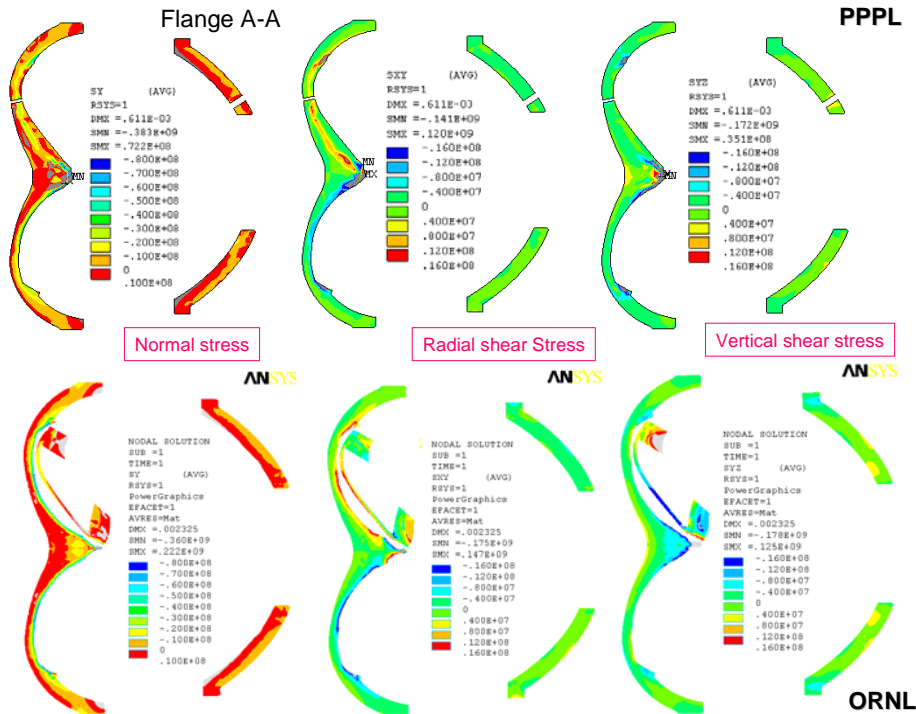


Fig 14: Normal Stresses and Shear Stresses for the Flange Spacer Elements at 0°

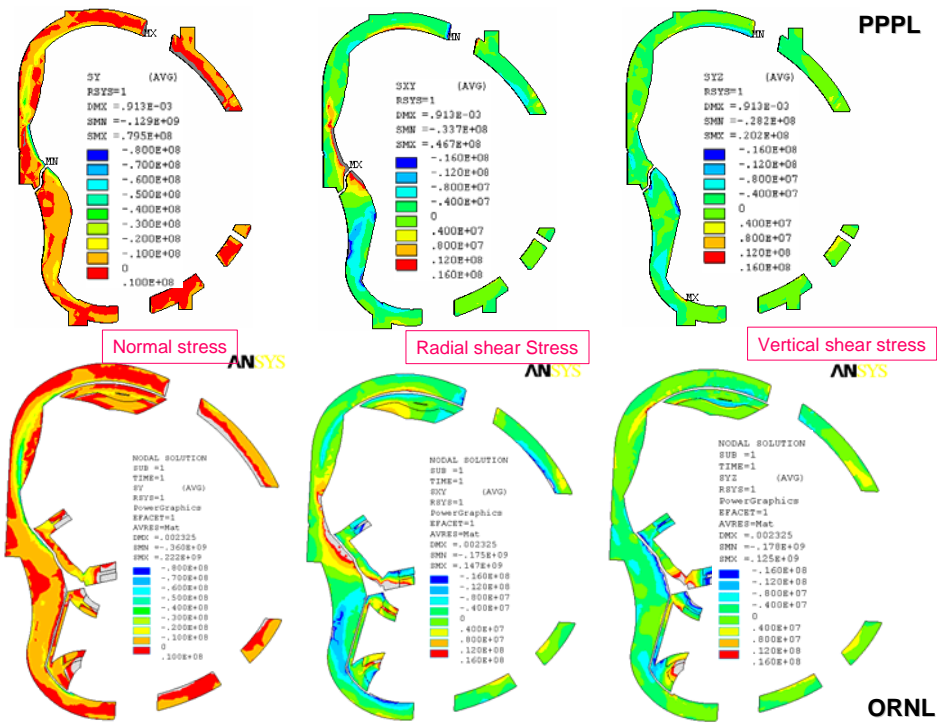


Fig 15: Normal Stresses and Shear Stresses for the Flange Spacer Elements at 20°

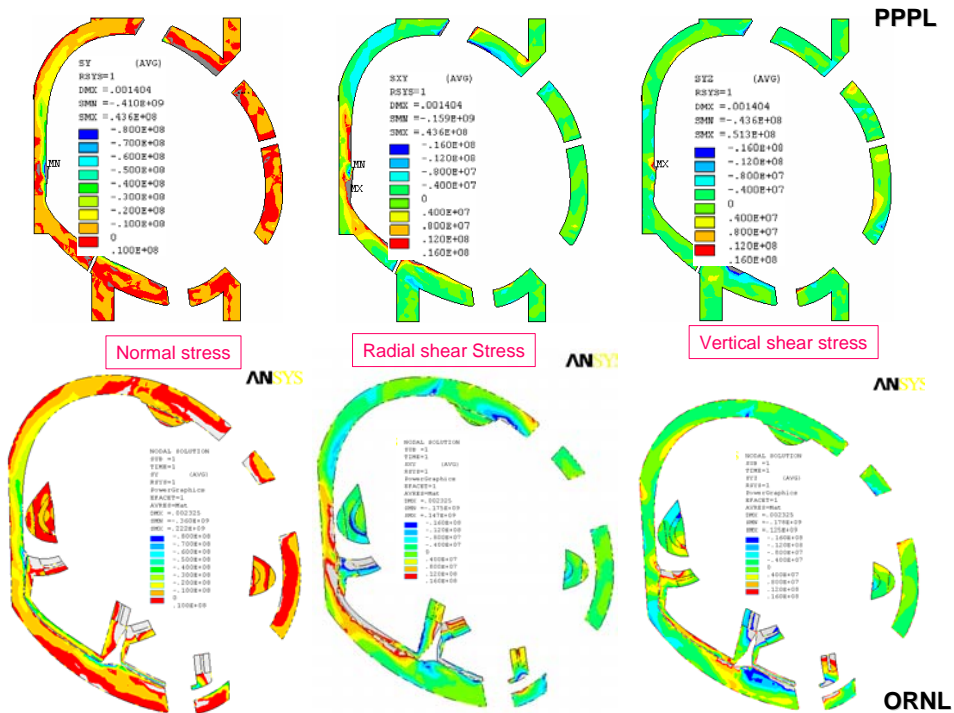


Fig 16. Normal Stresses and Shear Stresses for the Flange Spacer Elements at 40°

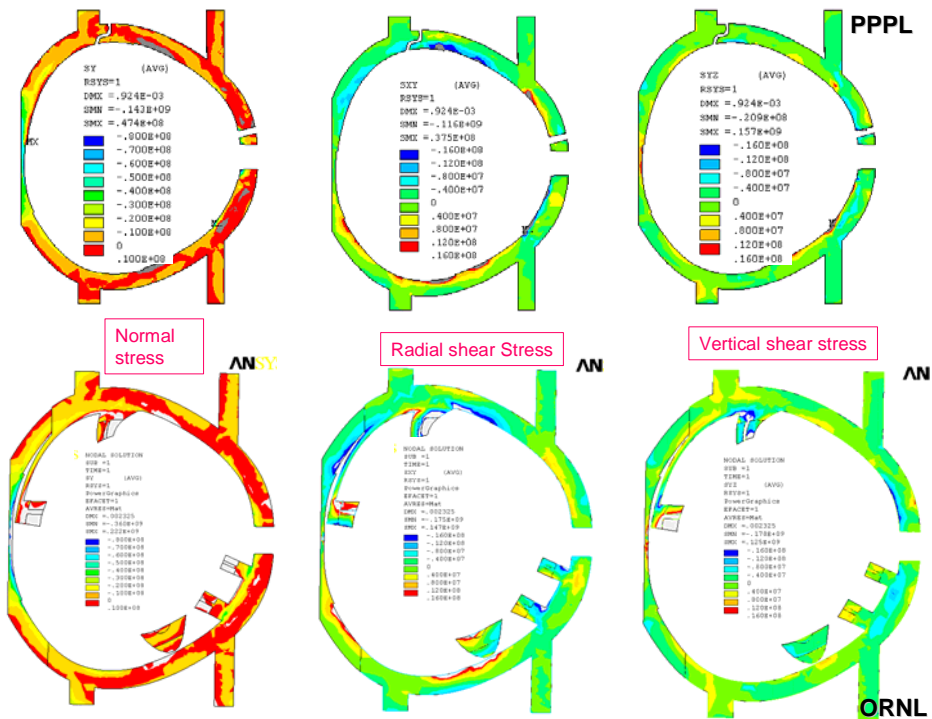


Fig. 17. Normal Stresses and Shear Stresses for the Flange Spacer Elements at 60°

#### IV. CONCLUSIONS AND FUTURE WORK

The following Conclusions are made based on the results of these two separate independent finite element analysis studies (Mechanica and ANSYS).

1. The allowable stress for the membrane plus bending will be 322.5 MPa, which is larger than the maximum stress of 283 which occurs on the BC interface near a geometric discontinuity. The peak stress on the tee structure, which occurs on the B coil shell, is about 175 MPa.
2. The maximum gap between the coil and the shell structure reported is 0.8 and occurred in the Mechanica study of coil C. The corresponding ANSYS value for the same coil was 0.6.
3. The Ansys models provide a great more detail into the behavior of the shell structure and yields an accurate deformed coil shape that does not rely on artificial constraints on the tee, which will be used by a physics code to predict the doing pulse plasma shape.
4. The stresses in the Mechanica runs are slightly higher than those from ANSYS. This is most likely due to the normal constraints placed on the clamps pads which help apply the preload to the clamps. Ansys ties the clamps directly to the shell instead of fixing them in a specific direction.
5. The maximum deflection in the shell is 2.6 mm which occurs on the type B on the leading edge of the tee near a wing transition.
6. The max winding stresses (Von Mises) are generally quite low ranging from 66 to 79 Mpa between the three coil types.

This analysis report serves as a check on the previously non-linear report produced by PPPL on the modular coil assembly. The two analysis utilize similar analysis paths and properties with the main difference being that PPPL choose to solve a 6 coil courser model with cyclic symmetric conditions and ORNL choose to analyze a 3 coil model with a finer mesh. The main difference between the two analysis result summaries is that PPPL shows somewhat larger peak stresses in the windings than the ORNL model. This is most likely due to the course 3X1 mesh of the mold coil (PPPL version) versus the 6X2 mesh of the ORNL analysis. The finer mesh allows for the peak stresses to be distributed more evenly and accurately. The shell and flange interface stresses are in good agreement between the two models.

This analysis only documents one load scenario to be used on the NCSX machine. Further analysis should be performed on the others for verification purposes. Further, the weld analysis and the analysis of the bolted joints between the modular coils are not considered here. They will be addressed in separate Dacs in the near future.

## REFERENCES

- [1] L. MYATT, D. E. WILLIAMSON and H.M. FAN, "Electromagnetic Linear Structural Analysis of the National Compact Stellarator Experiment (NCSX) Modular Coil System," 16<sup>th</sup> ANS Topical Meeting on the Technology of Fusion Energy, Madison WI, September 12-14, 2004.
- [2] W. REIERSEN, Modular Coils (WBS14) System Design Description, NCSX FDR, May 2004
- [3] ANSYS Inc, 275 Technology Drive, Canonsburg, PA 15317
- [4] W.D. CAIN, "MAGFOR: A Magnetics Code to Calculate Field and Forces in Twisted Helical Coils of Constant Cross-Section", 10<sup>th</sup> IEEE/NPSS Symposium on Fusion Engineering, 1983
- [5] PTC, 140 Kendrick Street, Needham, MA 02494
- [6] NCSX Product Specification, "Modular Coil Windings Forms", NCSX-CSPEC-141-03-10, November 15, 2005
- [7] H.M. Fan. "Nonlinear Analysis of Modular Coil and Shell Structure" NCSX-CALC-14-001-001, February 2006

## Appendix A: Reaction Forces on MCWF from TF-Induced Loads

To: Michael Kalish (PPPL)  
From: Leonard Myatt (Myatt Consulting, Inc.)  
Date: 2 June 2005  
Subject: Reaction Forces on MCWF from TF-Induced Loads

### 1.0 Executive Summary

Two existing ANSYS<sup>1</sup> models are used to determine the forces which must be carried by the Modular Coil Winding Form (MCWF) as a result of the loads developed by TF coil system. The hybrid model<sup>2</sup> is used to determine the vertical forces which develop when the TF support structure restrains the vertical displacements from cooldown (85K) and max-current operation (0.5 T). This is expected to be 18.2 kN/TF coil (top and bottom).

The global model<sup>3</sup> is then used to determine the reaction force distribution as the applied load enters the TF coil superstructure and enters the MCWF support points. This analysis shows that the four inboard support points per 120° sector carry 60% of the TF coil vertical load: ~17 kN each. The 12 outboard support points per 120° sector carry the remaining 40% of the vertical load, with maximum value of ~4 kN.

These forces can be used by to determine the impact of restraining vertical displacements at the top and bottom of the TF coils through structural attachments on the MCWF.

---

<sup>1</sup> ANSYS Release 9.0, UP20041104, INTEL NT, ANSYS, Inc., Canonsburg, PA.

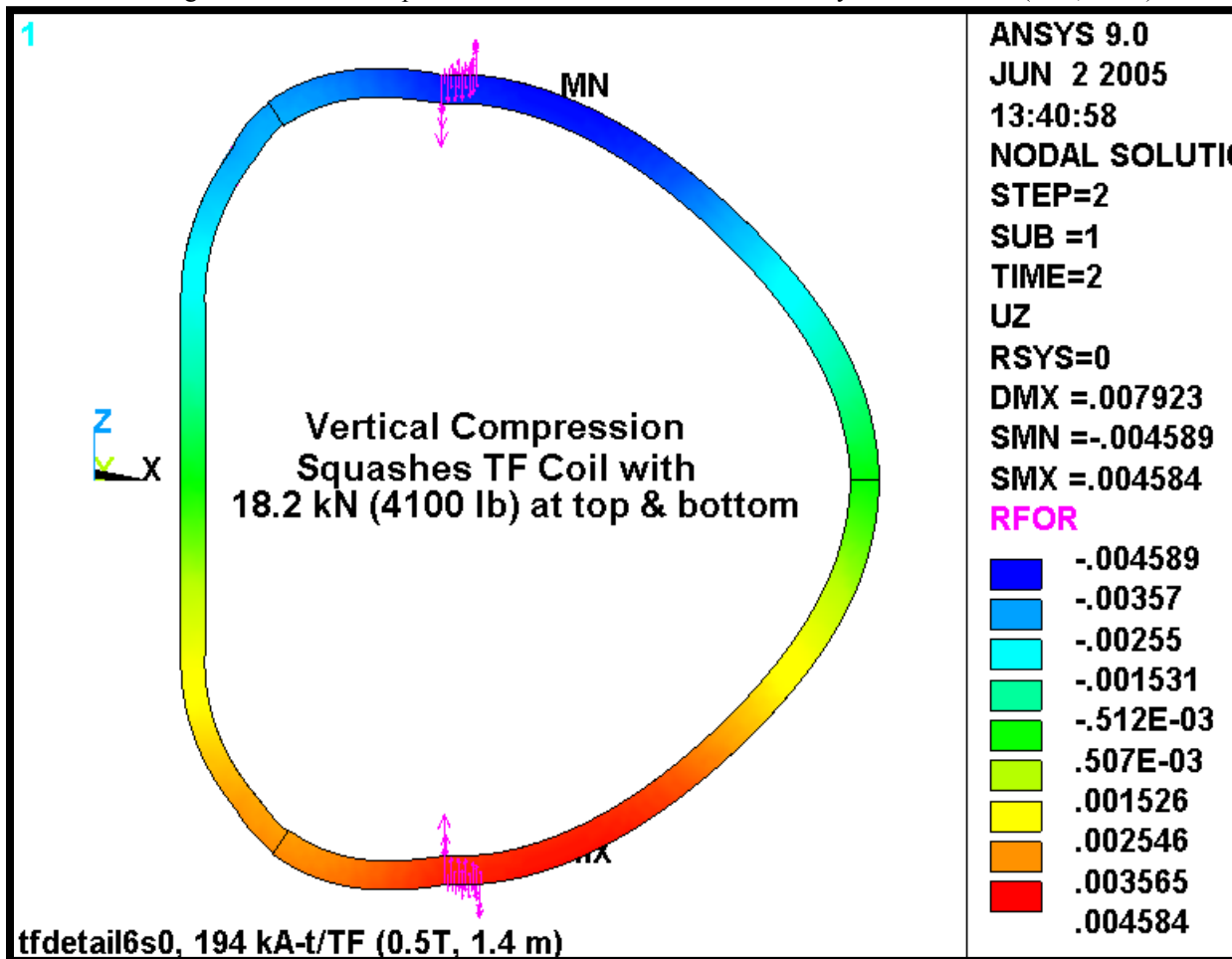
<sup>2</sup> Leonard Myatt, "Stress Analysis of the 3x4 Slip-Plane TF Coil with Cast SS Wedges," 16-May-05.

<sup>3</sup> Leonard Myatt, "Effects of Coil Support Concepts on TF WP Stresses," 16-May-05.

## 2.0 Analysis

The vertical forces developed by the vertical restraint of the TF coil are quantified by the hybrid model. Fig. 2.0-1 is a plot of the vertical displacement of TF winding pack (wedges excluded from plot) when the coil is cooled to 85K and energized to 0.5 T. So-called reaction force vectors are superimposed on the greatly deformed plot. Querying the database indicates that these vertical reaction forces sum to 18.2 kN on the top and bottom of each coil. It should be noted that some of the vectors point in the opposite direction compared to the majority. This is because the radial extent of the applied UZ boundary condition is slightly too big. However, it is reasonable to believe that the net vertical load is correct. This represents the most significant load which must ultimately be carried by the MCWF.

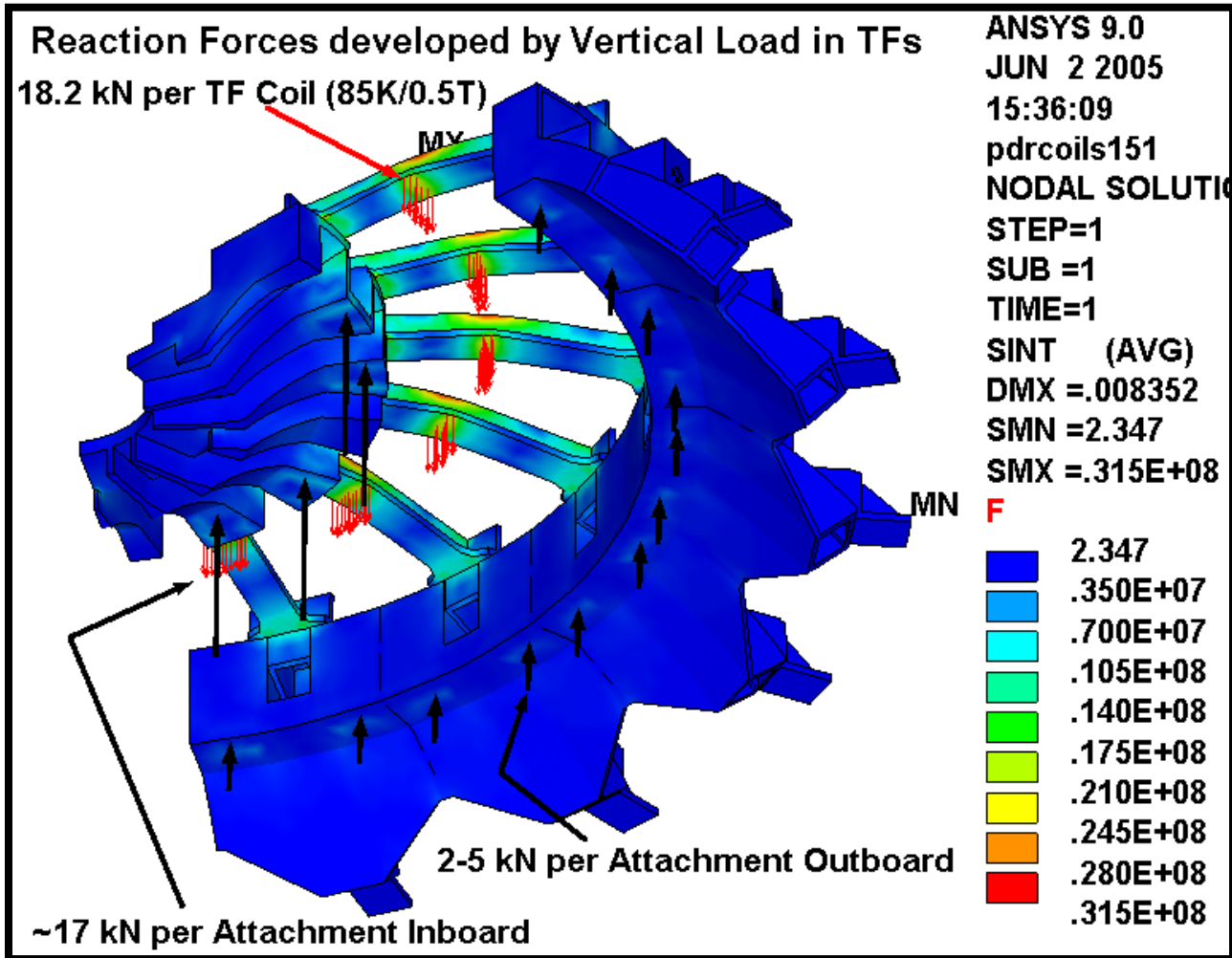
Fig. 2.0-1 Vertical Displacements and Reaction forces on the Hybrid Model WP (85K, 0.5 T)



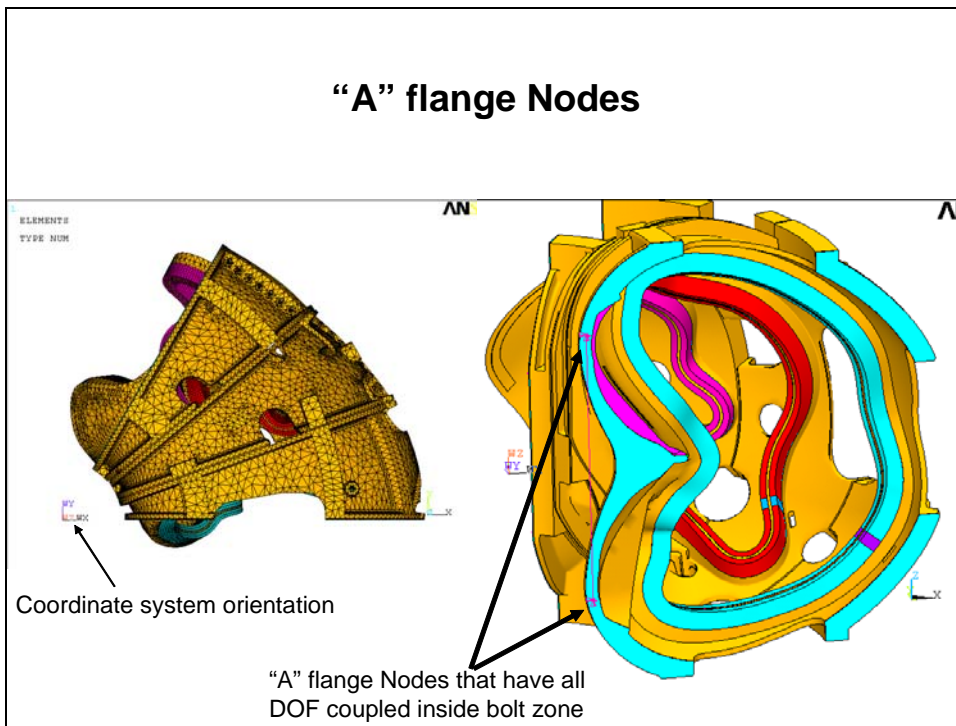
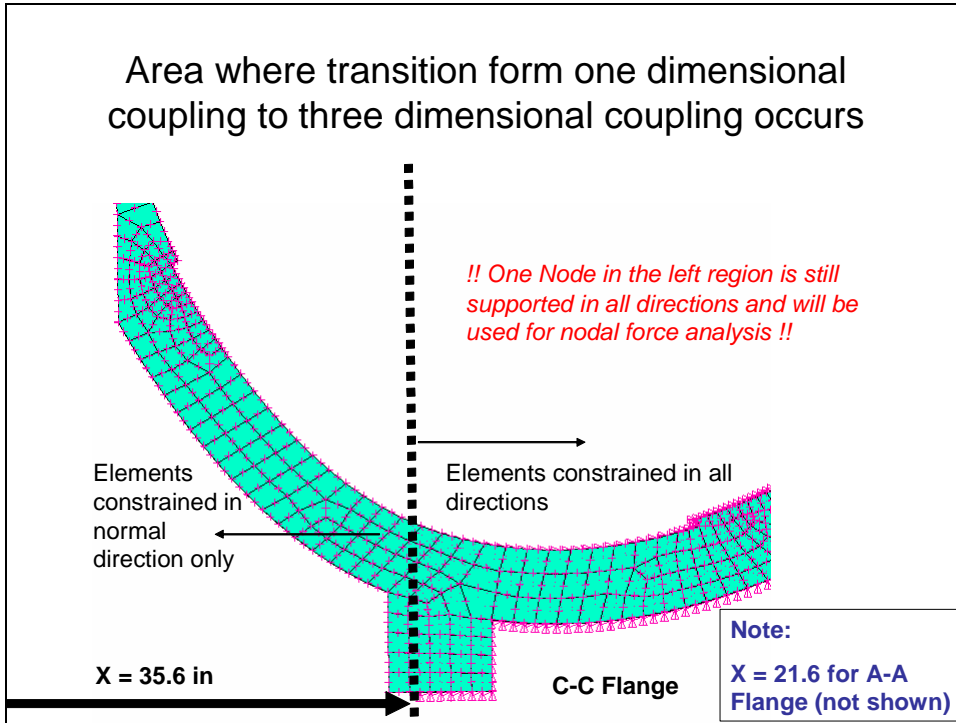
The vertical forces developed in the TF coil from 85k/0.5T operation must be transmitted through the coil support structure and into the MCWF. The global model has this load path fairly well defined, with the exception of the MCWF. The global model assumes that the MCWF provides a rigid restraint for the TF support structure.

Fig. 2.0-2 provides a graphical representation of the load distribution. The stress intensity in the support structure is contoured. Red vectors represent the 18.2 kN/TF applied load which is developed when the coils are restrained vertically at 85K and 0.5T. These come from the hybrid model as indicated in Fig. 2.0-1. The black vectors represent the reaction forces which are determined by this global model. They are simple representations of the more complex force distribution which is developed from anchoring nodal displacements in the bolting regions. Structural reaction forces are summed at each anchor point. On the inboard side, the distribution is rather uniform: 15.6+17.1+17.0+15.9 kN at the four anchor points in this 120° sector. These account for ~60% of the applied load. The outboard forces are much smaller and a bit more varied: 2.1+4.8+3.7+3.4+3.9+3.9+4.0+3.9+3.4+3.6+4.9+2.1 kN. These account for ~40% of the applied load.

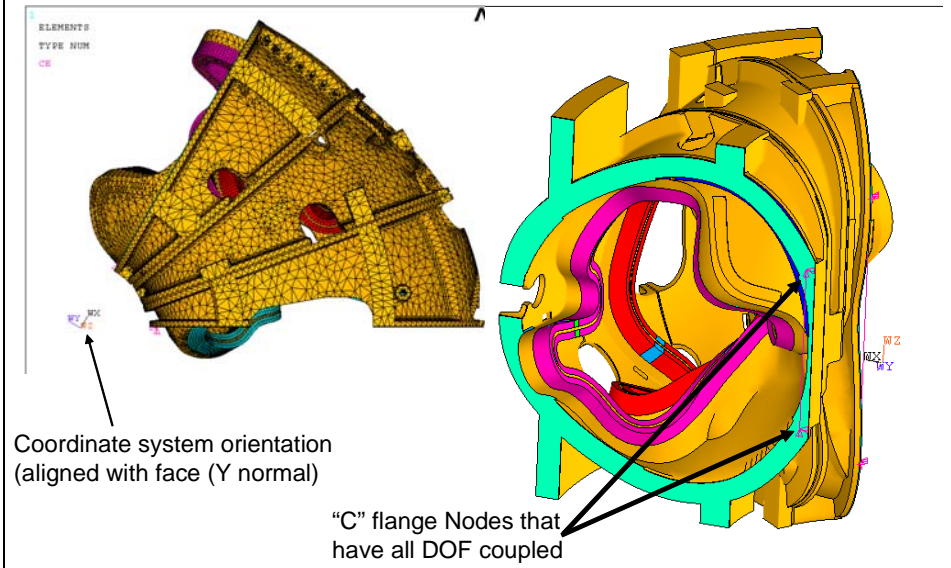
Fig. 2.0-2 TF Loads from Hybrid Model Distribute to MCWF through TF Support Structure



Appendix B: Consideration of using one bolt on inner leg to get total shear load:



## "C" flange Nodes



## Flange A: Force Results for the node pair

Force are in Newtons

- THE FOLLOWING X,Y,Z SOLUTIONS ARE IN THE GLOBAL COORDINATE SYSTEM

•

•	NODE	FX	FY	FZ
•	513516	-34636.	667.35	-10916.
•	524077	34636.	667.35	-10916.

- TOTAL VALUES

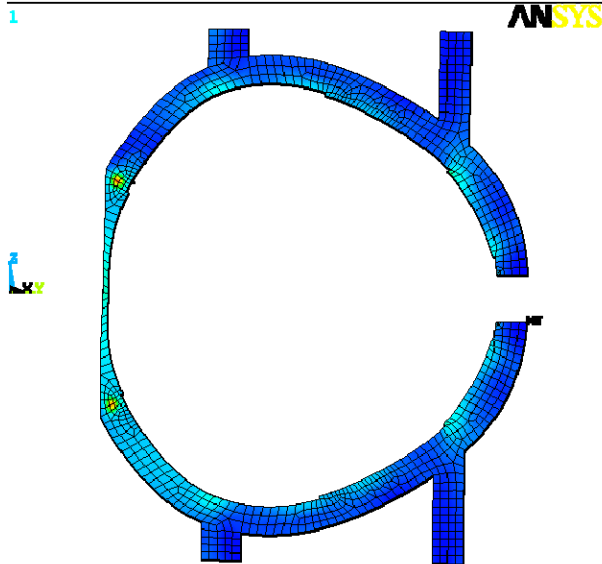
•	VALUE	0.66264E-03	1334.7	-21831.
---	-------	-------------	--------	---------

Note:

- ! Asymmetric nodes move in X together
- ! Asymmetric nodes move in opposite Y
- ! Asymmetric nodes move in opposite Z



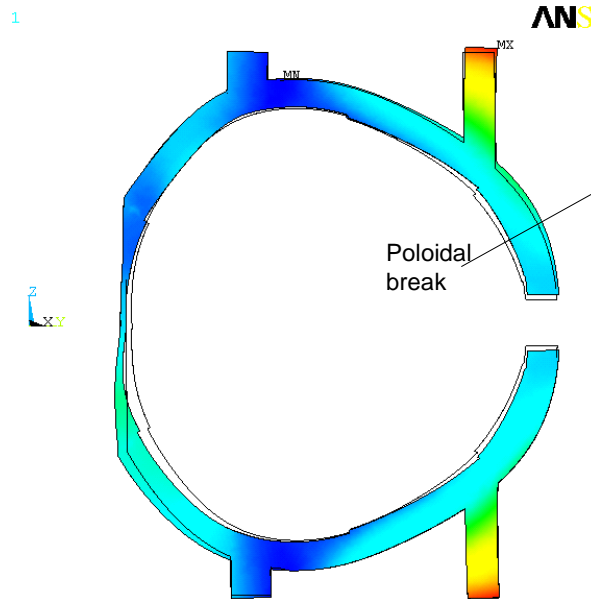
## Element Stress Intensity on Flange C-C (Average)



ANSYS  
 AVG ELEMENT NO:  
 STEP=1  
 SUB =1  
 TIME=1  
 SINT (AVG)  
 DMX = .003394  
 SMN = .165E+07  
 SMX = .301E+09  
 .165E+07  
 .349E+08  
 .682E+08  
 .101E+09  
 .135E+09  
 .168E+09  
 .201E+09  
 .234E+09  
 .268E+09  
 .301E+09

When looking at the element stress, the max value drops to around 32 ksi (clearly centered around the constrained nodes)

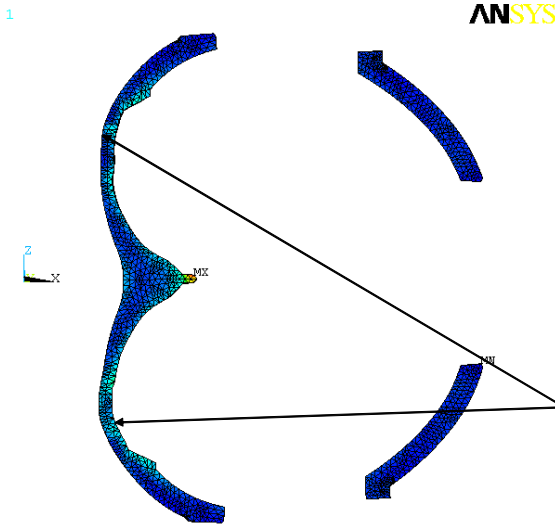
## Global Deflection of Flange C-C



ANSYS  
 NODAL SOLUTION  
 STEP=1  
 SUB =1  
 TIME=1  
 USUM (AVG)  
 RSYS=0  
 PowerGraphics  
 EFACET=1  
 AVRES=Mat  
 DMX = .810E-03  
 SMN = .518E-04  
 SMX = .810E-03  
 .518E-04  
 .136E-03  
 .220E-03  
 .304E-03  
 .389E-03  
 .473E-03  
 .557E-03  
 .641E-03  
 .725E-03  
 .810E-03

Poloidal break

# Element Stress Intensity on Flange A-A (Average)



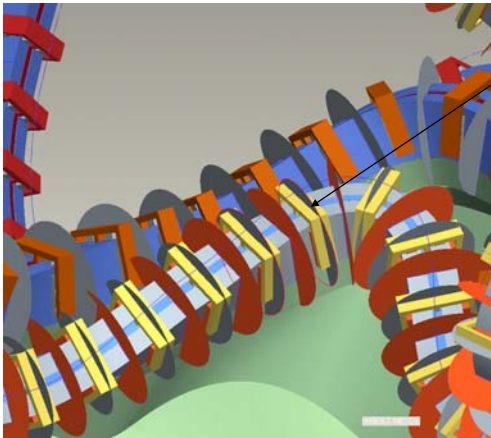
ANSYS  
AVG ELEMENT SO:  
STEP=1  
SUB =1  
TIME=1  
SINT (AVG)  
DMX =.393E-03  
SMN =849597  
SMX =.240E+09  
849597  
.274E+08  
.540E+08  
.806E+08  
.107E+09  
.134E+09  
.160E+09  
.187E+09  
.213E+09  
.240E+09

The nodal loads are not as obvious on this flange  
max stress is dominated by the midsection protrusion.

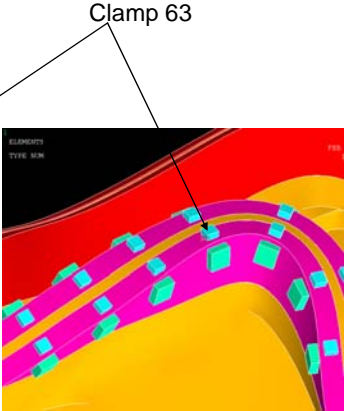


Appendix C Stresses Near Area of Clamp 63 on C Coil (DEMO of stress plots at every clamp.)

Location of Clamp



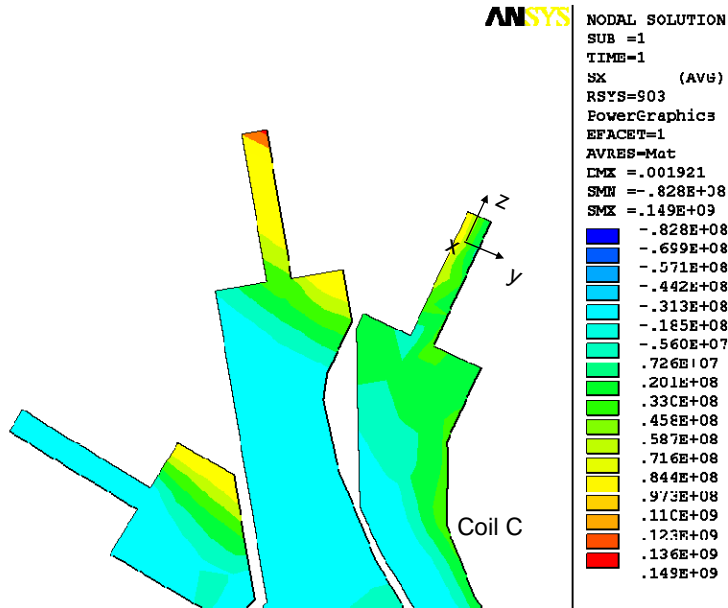
PROE



ANSYS

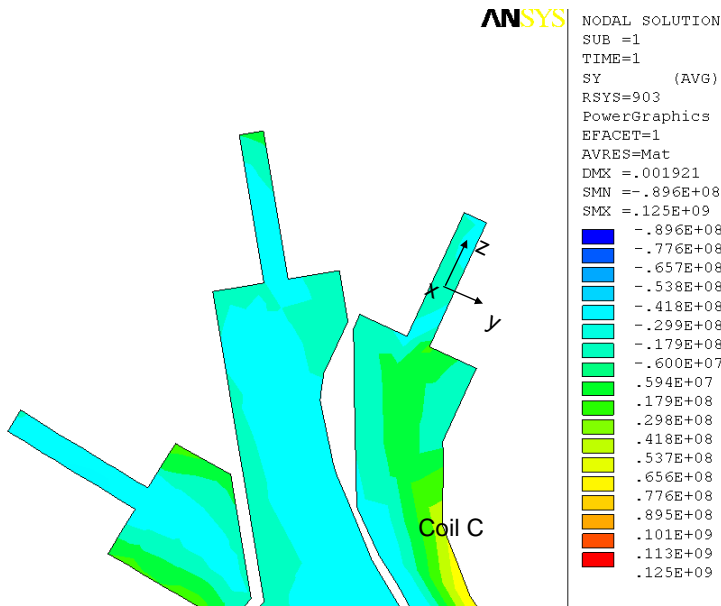
## X (Normal) Stress (Pa), though Clamp 63

1

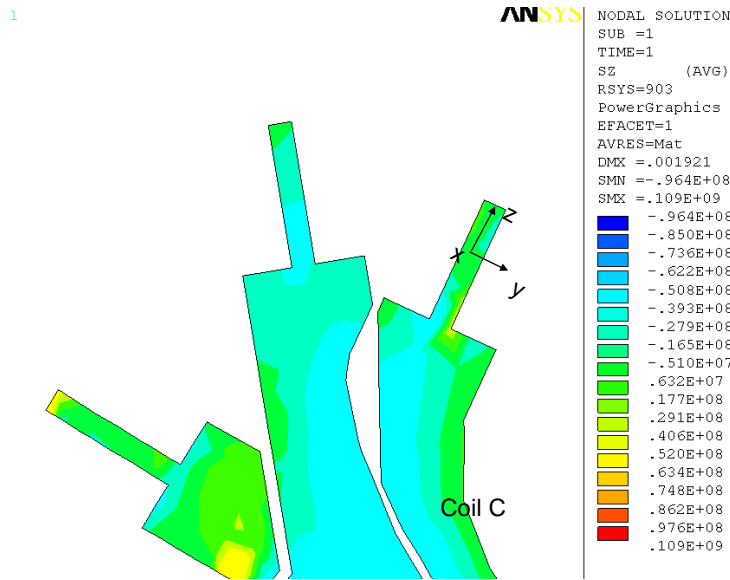


## Y Stress (Pa), though Clamp 63

1



## Z Stress (Pa), though Clamp 63



## Shear Stress Clamp 63

